Combining Tailored Ionic Liquids with $Ti_3C_2T_x$ MXenes for an Enhanced Load-Carrying Capacity under Boundary Lubrication

Philipp G. Grützmacher[1*], Roman Neuhauser[1], Kristof Stagel[2], Katharina Bica-Schröder[2], Guido Boidi[3], Carsten Gachot[1*], Andreas Rosenkranz[4*]

[1] Institute for Engineering Design and Product Development, Research Unit Tribology E307-05, TU Wien, 1060 Vienna, Austria
[2] Institut für Angewandte Synthesechemie (IAS), Sustainable Organic Synthesis and Catalysis research group, TU Wien, 1060 Vienna, Austria
[3] AC2T research GmbH, Viktor-Kaplan-Straße 2/C, Wiener Neustadt 2700, Austria
[4] Department of Chemical Engineering, Biotechnology and Materials (FCFM), Universidad de Chile, Santiago, Chile

Corresponding authors: Philipp G. Grützmacher (philipp.gruetzmacher@tuwien.ac.at), Carsten Gachot (carsten.gachot@tuwien.ac.at), Andreas Rosenkranz (arosenkranz@ing.uchile.cl)

Abstract

To improve the efficiency and lifetime of mechanical components, new lubrication systems are needed. Two complementary material classes, which have demonstrated a promising tribological performance, are ionic liquids and MXenes (2D transition metal carbides and nitrides). In this study, we used $Ti_3C_2T_x$ MXenes as additives in ionic liquids (ILs) to improve their load-carrying capacity under boundary lubrication. The specifically synthesized ILs share the same cation (trioctyl(methyl)phosphonium) but different anions (dimethyl phosphate and dibutyl phosphate for IL1 and IL2, respectively) to assess the effect of the anion's alkyl chain length. The wear reduction performance was tested with a cylinder-on-ring contact in a standardized Brugger tester, which is suitable to study boundary lubrication and to assess the anti-wear ability of the IL/MXene lubricant blends. MXenes indicate an excellent dispersibility in both ILs over 24 hours. It is found that, irrespective of the used IL, the addition of MXenes always increased the load-carrying capacity. Particularly, significantly reduced wear and thus

a high load-carrying capacity was observed for the combination IL2/MXenes, which also outperformed fully formulated commercially available lubricants such as turbine oils.

Keywords: Tribology; 2D Materials; MXenes; Ionic Liquids; Wear

Introduction

The ongoing climate crisis demands for more energy efficient mechanical systems, which will reduce the consumption of resources and emission of greenhouse gases. Consequently, this requires the development of new lubricants, which minimize friction and wear, are eco-friendly, and above all not based on crude oil [1][2].

Two material classes, which have great potential to be used as future lubricants due to their extraordinary tribological behaviour, are ionic liquids (ILs) and 2D materials [3]–[5]. ILs are molten salts in liquid state containing an organic cation and an anion, which can be either organic or inorganic [5][6]. There are numerous different cations and anions available, making the properties of ILs tuneable [5]. Furthermore, they possess an excellent thermal stability, high heat capacity, good electrical conductivity, and are often considered as eco-friendly materials due to their low volatility and non-flammability [7][8]. These properties give ILs various advantages over conventional liquid lubricants (oils and greases). The superior tribological performance has been firstly reported for an IL (1-methyl-3-hexylimidazolium tetrafluoroborate) by Ye et al. in 2001 [7]. Subsequently, numerous ILs have been synthesized and their excellent tribological behaviour as base lubricant or lubricant additive was systematically studied [9]. Several studies have also verified superlubricious states, i.e., a coefficient of friction (COF) below 0.01, when using ILs [10][11]. The lubricating mechanism of ILs is based on the formation of thin films (as thin as a monolayer) on the involved rubbing surfaces [5]. These films are either absorbed layers with a layered structure possessing a low shear strength [12] or protective layers induced by tribochemical reactions between the IL and the rubbing material surfaces [6]. The load-carrying capacity and anti-wear properties of ILs can be further enhanced by the addition of 2D layered materials, such as graphene [13], graphene oxide [14], or MoS_2 [15], thus improving the ILs' tribological performance particularly under severe conditions. The ionic nature of ILs often allows for a good dispersibility of nanomaterials in the IL base liquid, which is crucial for their tribological performance [13]. The 2D materials can be adsorbed onto the contacting surfaces, where they form low-shear tribo-layers, thereby protecting the surfaces from wear [16].

A rather new member of the 2D material family are MXenes, which are 2D layered transition metal carbides, nitrides, and carbonitrides based on MAX phases [17]. The structure of MXenes (general formula $M_{n+1}X_nT_x$) is composed of alternating layers of transition metal atoms (M) and carbon or nitrogen atoms (X), whereby the outer layers are always X atoms, which are terminated with functional groups (T_x), such as -O, -OH, and -F [18]. MXenes have been used

in energy storage [19], sensing [20], or catalysis [21]. However, their layer structure with reduced bonding strength between the layers renders MXenes also interesting for tribological applications [22]. MXenes' interlayer binding energy and, therefore, the friction between the layers is significantly influenced by the surface terminations [23][24], making it possible to tailor their tribological properties. MXenes have already demonstrated their promising tribological performance on the nanoscale [25][26], the laboratory scale [27][28], and even when used for lubricating machine elements [29]. They can be used as solid lubricant coatings [27][30], lubricious phase in composites [31], or lubricant additives [32]. Recently, it has been shown that synergistic effects are induced by combining lithium hexafluorophosphate-based ILs and molybdenum carbide (Mo_2CT_x) MXenes as lubricating additives [33]. In ball-on-disk tests, a protecting tribo-layer with low shear strength consisting of molybdenum- and phosphorous oxides intermixed with as-deposited MXenes was formed, which resulted in macroscale superlubricity (COF of 0.004) at contact pressures up to 1.42 GPa. While MXenes as solid lubricant coatings have been found to work well under medium contact pressures below 1 GPa, they are easily degraded when the contact pressures are too high, leading to reduced wear life [34]. Therefore, for severely loaded contacts, the combination with ILs can be beneficial, as MXenes are embedded into the IL-based tribo-layers, leading to a slower degradation and improved tribological performance. Based on the presented state-of-the art, it becomes evident that MXenes have been scarcely tested as lubricant additives in ILs. Considering the chemical diversity and tunability of both ILs and MXenes, we anticipate significant potential to optimize the resulting tribological performance when combining ILs with MXenes. Therefore, in this study, we investigate the tribological behaviour of $Ti_3C_2T_x$ MXenes as additives in two different ILs ($P8881(MeO)_2PO_2$ (**IL1**) and $P8881(BuO)_2PO_2$ (**IL2**), which are prepared in a halide-, chlorine-, and fluoride-free manner to avoid tribo-corrosion issues in the respective metal contacts. In this regard, multi-layer $Ti_3C_2T_x$ has been chosen since it is the most explored MXene in tribology and, therefore, serves as an excellent benchmark. The experiments are performed on a Brugger lubricant tester (DIN 51347-1), which is particularly suitable for studying boundary lubrication, thus allowing to assess MXenes' effect on the load-carrying capacity and anti-wear ability of IL-based lubricants. The results demonstrate that MXenes can improve the load-carrying capacity of ILs under extreme conditions. This is a crucial step for using the tunability of both involved materials to create tailored lubricants.

Materials and Methods

Synthesis and Characterization of MXene Nanosheets

Multi-layer $Ti_3C_2T_x$ nano-sheets were fabricated by selective etching of 2 g of MAX-Ti_3AlC_2 powder (purchased from Forsman Scientific Co. Ltd., Beijing, China) in 20 ml of highly concentrated hydrofluoric acid (HF) with a concentration of 40 wt.-%. The mixture of Ti_3AlC_2 powder and HF was stirred at a speed of 60 rpm and a temperature of 35 °C for 24 hours. After etching, the mixture was centrifuged at 3500 rpm and washed with deionized water in several washing cycles until a final pH of 6 was obtained and the residue was collected. Finally, the suspension was vacuum-filtrated and freeze-dried for 24 hours at -60 °C (pressure below 30 Pa).

The structure, quality, and interlayer distance of the as-synthesized multi-layer $Ti_3C_2T_x$ nano-sheets were characterized by transmission electron microscopy (TEM, Tecnai F20, FEI) using an acceleration voltage of 200 kV. To characterize their surface chemistry, Raman spectra were obtained applying a Witec Alpha 300 RA in backscattering geometry and an excitation wavelength of 532 nm. The spectra were acquired between 80 to 1000 cm^{-1} with an acquisition time of 128 s for each spectrum and a spectral resolution of 3 cm^{-1} using a 300 l/mm grating.

Synthesis of Ionic Liquids and Preparation of Lubricants

Two ILs, $P8881(MeO)_2PO_2$ (**IL1**) and $P8881(BuO)_2PO_2$ (**IL2**) were synthesized from the corresponding phosphines and alkyl phosphates in batch or continuous mode for optional scale-up. They share the same cation (trioctyl(methyl)phosphonium), while having dimethyl phosphate (DMP) anions and dibutyl phosphate (DBP) as anions in case of IL1 and IL2, respectively (**Figure 1**).

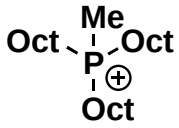

Cations of IL1 and IL2

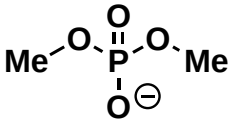

Anion of IL1

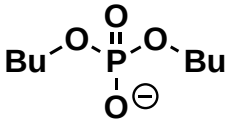

Anion of IL2

Figure 1. Chemical structures of the synthesized ionic liquids, namely P8881$(MeO)_2PO_2$ (**IL1**) and P8881$(BuO)_2PO_2$ (**IL2**). Both ionic liquids share the same cation (trioctyl(methyl)phosphonium (P8881)) but possess different anions; dimethyl phosphate (**DMP**) and dibutyl phosphate (**DBP**) for IL1 and IL2, respectively.

1) P8881$(MeO)_2PO_2$ (**IL1**)

As-synthesized and distilled trioctylphosphine (1.0 equiv.) was transferred to a round-bottom flask under argon atmosphere. Subsequently, trimethyl phosphate (1.2 equiv.) was added to the flask under continuous stirring. The temperature was increased stepwise to 140 °C, and the mixture was stirred under inert atmosphere for 72 hours. After completion of the reaction, the excess trimethyl phosphate was removed under vacuum (0.2 mbar, 95 °C). The desired product ($P8881(MeO)_2PO_2^-$) was obtained as an orange, viscous liquid at a yield of 98%.

In the future, ILs can be synthesized in a continuous manner (Vapourtec E-Series Flow Chemistry System) for scale-up. In this method a tube reactor is used, which is designed for high-temperature reactions. In the continuous process, a 25-mL Vapourtec high-temperature tube reactor is employed, operating at 240 °C. The two reactants are supplied to the reactor in a manner that an equimolar ratio is maintained during the reaction, with flow rates of 0.129 mL/min for trimethyl phosphate and 0.496 mL/min for trioctylphosphine, respectively. This corresponds to a residence time of 40 minutes. With the continuous method, a conversion of 75% is reached, and work-up can be performed accordingly.

2) P8881$(BuO)_2PO_2$ (**IL2**)

P8881$(BuO)_2PO_2$ is obtained in a subsequent synthesis step using IL1 as reaction product. A round-bottom flask was charged with (P8881$(MeO)_2PO_2$) (1.0 eq.) and dibutyl phosphate (1.2 eq.) under argon atmosphere. Afterwards, triethylamine (1.4 eq.) was added dropwise under cooling in an ice bath. After the addition was complete, the reaction mixture was stirred for 20 minutes at 0 °C and overnight at room temperature. Distilled water was then infused to the mixture, before vigorously stirring it for 16h at room temperature. The mixture was transferred in a separatory funnel and washed one time with a mixture of triethylamine and distilled water (10:90 v/v) and 4 times with distilled water. Finally, the residual water was removed under vacuum (0.2 mbar, 95 °C). The desired ionic liquid P8881$(BuO)_2PO_2$ was obtained as a slightly yellowish, viscous liquid with a yield of 97%.

The viscosities of IL1 and IL2 were evaluated at 40 and 100 °C (**Table 1**). For 40 °C, **IL1** showed a kinematic viscosity of 496 cSt. At 100 °C, the viscosity drastically dropped to 32 cSt. **IL2** had a lower kinematic viscosity of 223 cSt at 40 °C and 20 cSt at 100 °C, respectively.

Table 1. Kinematic viscosities of the ionic liquids (IL1 and IL2) measured at 40 and 100 °C.

Ionic liquid	Viscosity @ 40 °C (cSt)	Viscosity @ 100 °C (cSt)
IL1	496	32
IL2	223	20

For the tests with MXene additives, dispersions with a MXene concentration of 0.5 wt.-% in the ILs were prepared, which is a concentration typically used for solid lubricant additives [35]. The dispersions were mixed using a magnetic stirrer for 15 minutes followed by ultrasonication for 20 minutes to ensure a homogeneous dispersion. The dispersion stability was controlled by visual inspection in time intervals of 15, 30, 60, and 120 min as well as after 1440 min (24 h).

Tribological Experiments

The tribological performance of the ILs **with** and **without** $Ti_3C_2T_x$ under boundary lubrication was studied using a standardized Brugger tribometer according to the aforementioned DIN 51347-1. The test provides information on the lubricant's load-carrying capacity under pure sliding conditions at room temperature. The experimental conditions allow for the suitabilty of the used lubricant system under severe test conditions and due to the use of a standardized test the results can be compared to those available in the literature. The contact is established between a fixed cylinder (AISI 52100) with a diameter of 18 mm and a rotating ring (AISI D6) with an outer diameter of 25 mm (**Figure 2**). Prior to the test, 8 ml of the test lubricant is poured onto the ring surface. Due to the high viscosity of the ILs, a thick film formed on the entire surface of the ring. Afterwards, a constant load F_N of 400 N is applied (equivalent to an initial Hertzian contact pressure of 1.4 GPa) and the ring rotates with a constant speed of 960 r/min for 30 s, being equivalent to 1.2 m/s. After a lubricant-dependent run-time period, steel-steel contact occurs, simulating an oil starvation period. As a result, a well-defined elliptical wear scar is generated on the fixed cylinder with the major axis *a* and minor axis *b* in x- and y-direction (**Figure 2**). The performance of a lubricant is evaluated by analysing the contact area that expands linearly with time and is inversely proportional to the load-carrying capacity of

the tested lubricants [36]. To determine the contact area and the dimensions of the major and minor axis (*a* and *b*), a laser scanning confocal microscope (Keyence VK-X1000 3D) is used. Equation (1) is used to calculate the Brugger load-carrying capacity *B* (N/mm^2) of the tested lubricants. Three repetitions were carried out under the same test conditions to calculate an average load-carrying capacity.

$$B = \frac{4 \cdot F_N}{a \cdot b \cdot \pi} \quad (1)$$

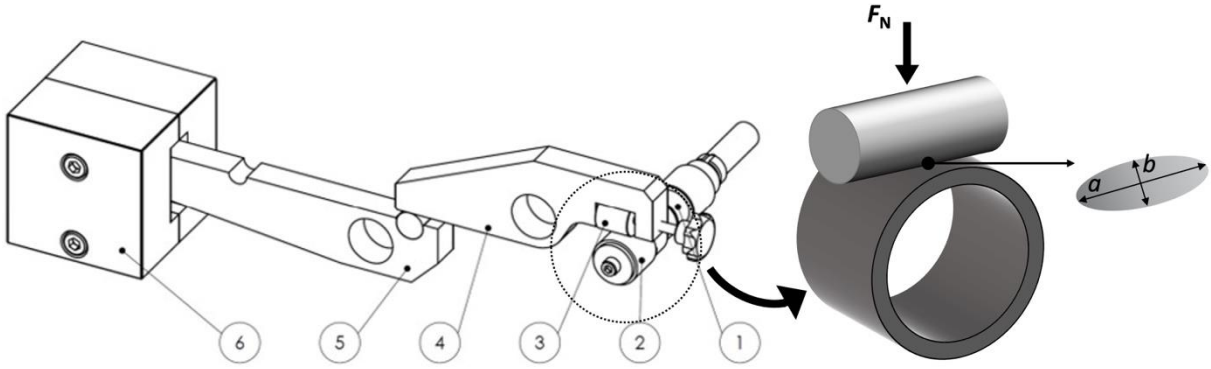

Figure 2. Schematic representation of the contact configuration of the Brugger tests and the resulting elliptical wear track on the cylinder with the major and minor axes *a* and *b*. (1) drive shaft, (2) rotating ring, (3) clamped cylinder, (4) sample lever, (5) load lever and (6) "dead" weight.

Results and Discussion

As confirmed by TEM, the used synthetic approach resulted in multi-layer $Ti_3C_2T_x$ flakes with an interlamellar spacing of 0.91 ± 0.09 nm (**Figure 3**(**a**) and (**b**)). These values align well with published data in literature [27]. The selected area electron diffraction (SAED) pattern (inset in **Figure 3**(**b**)) confirmed the hexagonal structure of the multi-layer $Ti_3C_2T_x$ [37]. Raman spectroscopy (**Figure 3**(**c**)) was conducted to obtain more information about their surface chemistry. The Raman spectrum of the as-synthesized $Ti_3C_2T_x$ showed vibrational modes at 160, 220, and 707 cm^{-1}, as well as broader peaks around 285, 376, and 600 cm^{-1}, which are associated with the respective -O, -OH, and -F surface terminations. The obtained Raman peaks correlate well with data published in literature [38].

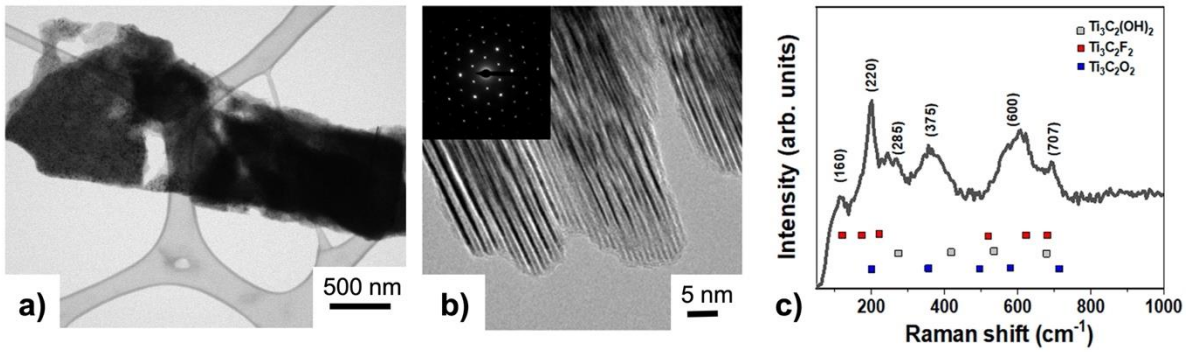

Figure 3. TEM-micrographs in (a) low- and (b) high-resolution (c) with the corresponding Raman spectrum of the as-synthesized multi-layer $Ti_3C_2T_x$.

Prior to tribological testing, the stability of the dispersions was inspected (**Figure 4**) since this aspect has been shown to significantly affect the tribological properties of lubricants with MXenes [39]. Visual inspection of the as-prepared ILs and MXene dispersions did not show any sign of MXene precipitation or sedimentation neither in IL1 nor in IL2 up to 24 h (1440 minutes). Therefore, it can be concluded that the compatibility between $Ti_3C_2T_x$ and the used ILs is excellent. Although the used ILs are hydrophobic, their intrinsic ionic nature results in strong electrostatic interactions with the polar MXenes [40]. Moreover, MXenes contain reactive -OH groups on their surface. Negatively charged ions are known to interact with H-containing bonds, resulting in the formation of a charge-induced hydrogen bond [41]. The IL's anion may interact with the MXenes' polar O-H bond in such a manner, thus enhancing the interaction between ILs and MXenes, leading to an enhanced dispersibility. Additionally, both ILs are highly viscous, which prevents re-agglomeration and sedimentation of MXenes after dispersion, thus also contributing to their excellent dispersibility [42]. Overall, we conclude that an influence of re-agglomeration and reduced dispersion stability over time on the tribological behaviour of the ILs with MXene additives is negligible.

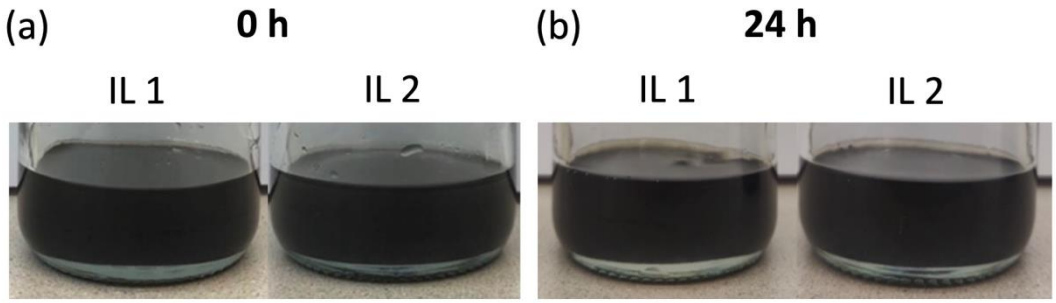

Figure 4. MXene dispersion in the ionic liquids IL1 and IL2 (a) directly after stirring and ultrasonication and (b) after 24 hours.

The tribological properties of the ILs with and without MXenes are studied on a Brugger tester, simulating high pressure conditions (boundary lubrication). The elliptical wear scars formed during the tests on the upper cylinders are shown in **Figure 5**. Apart from the dimensions of the wear scars, their appearance is similar independent of the lubricant used with signs of abrasive and adhesive wear. The high load applied during the tests results in boundary lubrication conditions with predominant solid-solid contact, which is clearly demonstrated by the significant wear of the cylinder surfaces. However, based on the reduced dimensions of the wear scar, a higher wear resistance can be observed for IL2 compared to IL1, while the addition of MXenes also positively influenced the resulting performance.

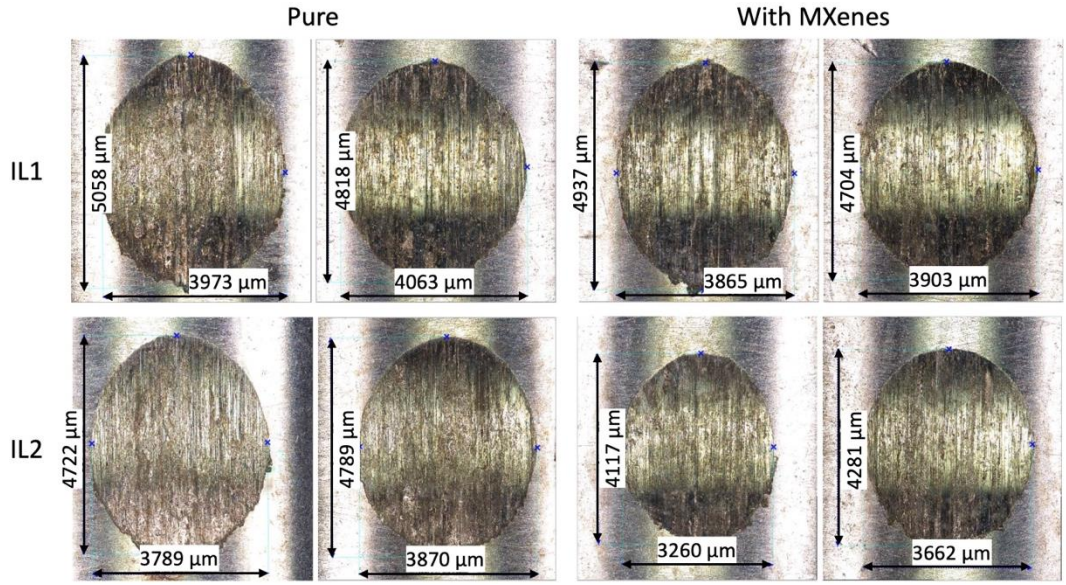

Figure 5. Wear scars on the cylinders after the Brugger test with the ionic liquids IL1 and IL2 with and without $Ti_3C_2T_x$ additives (pure, images on the left). From the dimensions *a* and *b* of the wear scars, the Brugger load-carrying capacity is determined according to equation 1. Two different wear scars are shown for all lubricant formulations, showing a good reproducibility of the tests.

The wear resistance under high pressure conditions is further evaluated with respect to the Brugger load-carrying capacity (**Figure 6**). As the load-carrying capacity is determined by dividing the applied normal load by the area of the wear scar, a higher load-carrying capacity implies a better wear resistance. The average load-carrying capacities for the pure IL1 and IL2 are 25.7 and 28.0 N/mm^2, respectively. These values are substantially higher than that of a non-additivated FVA2 base oil as well as comparable to fully-formulated and commercially-used turbine oils measured using the same test setup [6][36]. We already demonstrated the effectiveness of ILs to improve the anti-wear properties of a FVA2 base oil when used as additives with a concentration of 5 wt.-%, which was attributed to the formation of a phosphate-rich tribo-layer [6]. The pure ILs slightly increased the load-carrying capacity compared to the IL additivated base oils. We trace this observation back to their high viscosity promoting a thicker lubricant film as well as the greater availability of phosphorous-based compounds to form beneficial tribo-layers. This is supported by the fact that ILs have shown to readily form tribo-layers due to their inherent polarity, which facilitates self-adsorption [43].

Based on our results, **IL2** containing the anion with the butyl groups performs better than **IL1** (anion with methyl groups). This contradicts previous studies with these ILs showing a better performance for anions having shorter alkyl chain lengths due to quicker reactions of these anions with the surface leading to the formation of tribo-layers [6][44]. However, the applied load in [44] was also by two orders of magnitudes lower than in our study and, therefore, cannot be

easily compared to our study. Consequently, we anticipate that the potentially lower reactivity of IL2 is advantageous under the high applied load in our study, thus promoting a slower degradation of the IL and a longer lifetime (wear life). Additionally, it has been shown that the thickness and compactness of the formed IL-based tribo-layers mainly depends on the alkyl chain lengths of the ions [43][45][46]. Therefore, we hypothesize that IL2 can form a thicker and more compact tribo-layer on the steel surface, which protects the underlying surface from wear and results in a higher load-carrying capacity. This is somewhat counterintuitive since the viscosity of IL2 is significantly lower than that of IL1 (**Table 1**), basically suggesting a thinner lubricant film for IL2. However, under high-load conditions inducing locally high temperatures, the predominant lubrication regime for both ILs is boundary lubrication irrespective of their viscosity. Due to the expected low film thicknesses, the different viscosities only play a minor role regarding the resulting tribological performance.

For both ILs, the addition of multi-layer $Ti_3C_2T_x$ further improved the load-carrying capacity to 27.2 and 35.3 N/mm^2 for IL1+MXene and IL2+MXene, respectively. For IL2 in particular, this corresponds to values that are significantly higher than those of some fully formulated turbine oils used in helicopter applications [36]. We anticipate that this improvement is due to the additional formation of a MXene-rich tribolayer, which protects the steel surface from wear. The addition of MXenes had a greater effect for IL2, for which the load-carrying capacity increased by 26 % compared to a rather marginal improvement of 6 % for IL1. To understand this aspect, several elements have to be taken into consideration. As discussed above, we assume that IL2 has the capability to form a thicker and more compact wear-resistant tribo-layer. Therefore, the acting mechanical stress on the MXenes, which are an integral part of this layer, is reduced, leading to a slower MXene degradation (structural and chemical) and, thus a better performance. In this context, it has been shown that MXene tribo-layers degrade rapidly under high contact pressures of 1.47 GPa [34], which are close to the initial contact pressure of 1.4 GPa in our experiments, reducing their beneficial effects. Additionally, MXenes' mobility in the liquids depends on their viscosity [47]. The lower viscosity of IL2 (**Table 1**) could benefit the mobility of MXenes in the ionic liquid. Therefore, the tribological contact is provided more easily with MXenes, which are embedded into the hybrid IL/MXene tribo-layer to reduce wear.

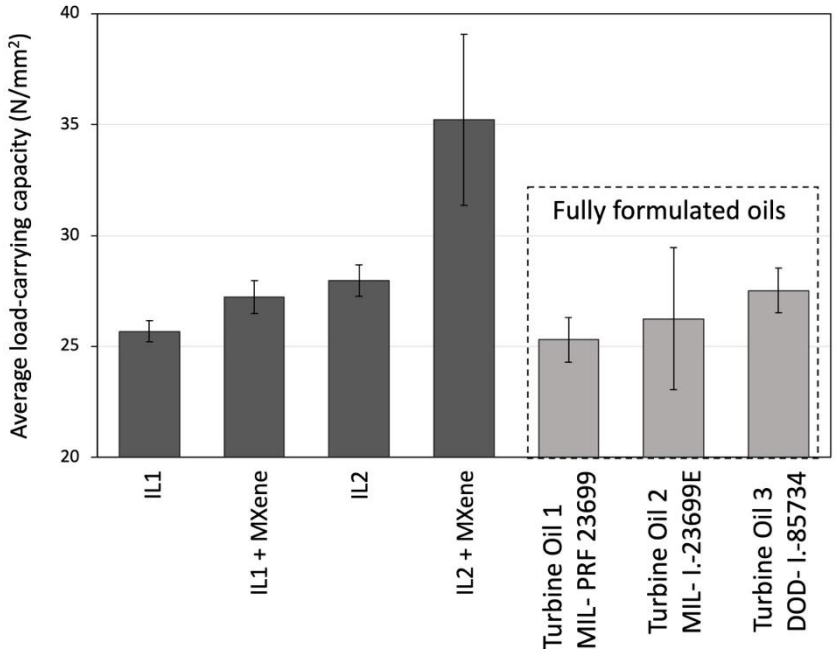

Figure 6. Average Brugger load-carrying capacity for the pure ILs 1 and 2 as well as the ILs additivated with 0.5 wt.-% of MXenes. As a comparison, the average Brugger load-carrying capacity of fully formulated turbine oils is provided [36].

Conclusions

In this work, we presented a new lubrication system consisting of ILs and $Ti_3C_2T_x$ acting as additive (concentration of 0.5 wt.-%) with the overall purpose to enhance the load carrying capacity and thus finally wear resistance under boundary lubrication at relatively high loads of 400 N. The specifically synthesized ILs share the same cation (trioctyl(methyl)phosphonium) but anions with different alkyl chain lengths (dimethyl phosphate and dibutyl phosphate for IL1 and IL2, respectively).

MXenes showed an excellent dispersibility in both applied ILs over 24 hours, which was attributed to the intrinsic ionic nature of the ILs favouring electrostatic interactions with the polar MXenes, possible formation of hydrogen bonds between the negatively charged ions and OH-containing terminations of MXenes, as well as the high viscosity of the ILs preventing re-agglomeration.

The produced IL/MXene dispersions always resulted in a higher average load-carrying capacity in standardized Brugger tests compared to the pure ILs. The combination IL2/MXene demonstrated the highest average load-carrying capacity, corresponding to an increase by 26 % compared to the pure IL. The excellent tribological performance induced by the IL/MXene dispersion was explained by the formation of hybrid tribo-layers on the rubbing surfaces, which

protect the surfaces from wear. Anions with longer alkyl chain lengths are known to form thicker tribo-layers, which explains the better performance of IL2, especially in combination with MXenes. The MXenes in the IL2 tribo-layer are exposed to less stress compared to IL1, resulting in a slower degradation and, consequently, improved wear resistance. It is worth to emphasize that the combination IL2/MXene even outperformed fully formulated turbine oils regarding their load bearing capacity and wear-resistance under contact pressures of 1.4 GPa. The results of our work point towards the suitability of eco-friendly IL/MXene lubricants with high thermal stability for high-load applications.

Authors contribution

P. G. Grützmacher, C. Gachot, and A. Rosenkranz conceptualized the work. K. Stagel fabricated the ionic liquids. R. Neuhauser performed the tribological experiments and the wear analysis. P. G. Grützmacher, C. Gachot, A. Rosenkranz and K. Bica-Schröder analyzed the data. P. G. Grützmacher, R. Neuhauser, G. Boidi, and A. Rosenkranz visualized the data. P. G. Grützmacher and A. Rosenkranz prepared the first draft of the manuscript. P.G. Grützmacher, K. Stagel, K. Bica-Schröder, C. Gachot, and A. Rosenkranz edited the manuscript. All authors provided suggestions for the final discussion, have reviewed, edited, and read the final version of the manuscript.

Funding Sources

Fondecyt 1220331

EQM 190057

InTribology1 872176

Notes

Authors approve ethics in publishing and consent to participate thereof.

The authors declare consent for publication.

Authors declare no competing interests.

Acknowledgement

A. Rosenkranz gratefully acknowledges the financial support given by ANID-CONICYT within the projects Fondecyt 11180121 and Fondequip EQM190057. G. Boidi thanks the “Austrian COMET-Programme” (Project InTribology1, no. 872176) for the financial support.

Conflict of Interest

Authors declare no conflict of interest.

Table of content

To develop new lubrication concepts, the combination of ionic liquids and multi-layer $Ti_3C_2T_x$ was tested under boundary lubrication with the overall aim to improve their load-carrying capacity. Significantly reduced wear and a higher load-carrying capacity was verified for the combination IL2/MXenes, which even outperformed fully formulated commercially available turbine oils.

Philipp G. Grützmacher, Roman Neuhauser, Kristof Stagel, Katharina Bica-Schröder, Guido Boidi, Carsten Gachot, Andreas Rosenkranz

Combining Tailored Ionic Liquids with $Ti_3C_2T_x$ MXenes for an Enhanced Load-Carrying Capacity under Boundary Lubrication

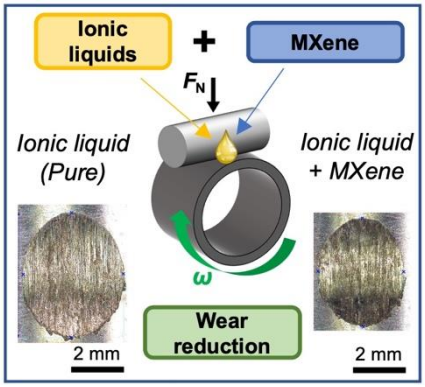

For Table of Contents Use Only.

References

[1], Eds: B.K. Sharma, G. Biresaw, *Environmentally Friendly and Biobased Lubricants*, CRC Press**2016**.

[2] K. Holmberg, A. Erdemir, *Friction* **2017**, *5*, 263.

[3] S. Zhang, T. Ma, A. Erdemir, Q. Li, *Materials Today* **2019**, *26*, 67.

[4] I. Minami, *Molecules* **2009**, *14*, 2286.

[5] H. Xiao, *Tribology Transactions* **2017**, *60*, 20.

[6] A. Anifa Mohamed Faruck, P.G. Grützmacher, C.-J. Hsu, D. Dworschak, H.-W. Cheng, M. Valtiner, K. Stagel, P. Mikšovsky, A.R. Sahoo, A. Sainz Martinez, K. Bica-Schröder, M. Weigand, C. Gachot, *Friction* **2022**.

[7] C. Ye, W. Liu, Y. Chen, L. Yu, *Chemical Communications* **2001**, *21*, 2244.

[8] M.D. Avilés, N. Saurín, T. Espinosa, J. Sanes, J. Arias-Pardilla, F.J. Carrión, M.D. Bermúdez, *Express Polym Lett* **2017**, *11*, 219.

[9] Y. Zhou, J. Qu, *ACS Appl Mater Interfaces* **2017**, *9*, 3209.

[10] X. Ge, J. Li, C. Zhang, Y. Liu, J. Luo, *ACS Appl Mater Interfaces* **2019**, *11*, 6568.

[11] X. Ge, J. Li, C. Zhang, Z. Wang, J. Luo, *Langmuir* **2018**, *34*, 5245.

[12] S. Perkin, T. Albrecht, J. Klein, *Phys. Chem. Chem. Phys.* **2010**, *12*, 1243.

[13] V. Khare, M.Q. Pham, N. Kumari, H.S. Yoon, C.S. Kim, J. Il Park, S.H. Ahn, *ACS Appl Mater Interfaces* **2013**, *5*, 4063.

[14] X. Ge, J. Li, H. Wang, C. Zhang, Y. Liu, J. Luo, *Carbon N Y* **2019**, *151*, 76.

[15] K. Gong, W. Lou, G. Zhao, X. Wu, X. Wang, *Friction* **2020**, *8*, 674.

[16] P.C. Uzoma, H. Hu, M. Khadem, O. V. Penkov, *Coatings* **2020**, *10*.

[17] B.C. Wyatt, A. Rosenkranz, B. Anasori, *Advanced Materials* **2021**, *2007973*, 1.

[18] A. VahidMohammadi, J. Rosen, Y. Gogotsi, *Science* **2021**, *372*.

[19] B. Anasori, M.R. Lukatskaya, Y. Gogotsi, *Nat Rev Mater* **2017**, *2*.

[20] S.J. Kim, H.J. Koh, C.E. Ren, O. Kwon, K. Maleski, S.Y. Cho, B. Anasori, C.K. Kim, Y.K. Choi, J. Kim, Y. Gogotsi, H.T. Jung, *ACS Nano* **2018**, *12*, 986.

[21] A. Liu, X. Liang, X. Ren, W. Guan, M. Gao, Y. Yang, Q. Yang, L. Gao, Y. Li, T. Ma, *Adv Funct Mater* **2020**, *30*, 2003437.

[22] D. Zhang, M. Ashton, A. Ostadhossein, A.C.T. Van Duin, R.G. Hennig, S.B. Sinnott, *ACS Appl Mater Interfaces* **2017**, *9*, 34467.

[23] E. Marquis, M. Cutini, B. Anasori, A. Rosenkranz, M.C. Righi, *ACS Appl Nano Mater* **2022**.

[24] Q. Yang, S.J. Eder, A. Martini, P.G. Grützmacher, *Npj Mater Degrad* **2023**, *7*, 6.

[25] A. Rodriguez, M.S. Jaman, O. Acikgoz, B. Wang, J. Yu, P.G. Grützmacher, A. Rosenkranz, M.Z. Baykara, *Appl Surf Sci* **2021**, *535*, 147664.

[26] P. Serles, M. Hamidinejad, P.G. Demingos, L. Ma, N. Barri, H. Taylor, C.V. Singh, C.B. Park, T. Filleter, *Nano Lett* **2022**, acs. nanolett.2c00614.

[27] P.G. Grützmacher, S. Suarez, A. Tolosa, C. Gachot, G. Song, B. Wang, V. Presser, F. Mücklich, B. Anasori, A. Rosenkranz, *ACS Nano* **2021**, *15*, 8216.

[28] J.Y.A. Hurtado, P.G. Grützmacher, J.M. Henríquez, D. Zambrano, B. Wang, A. Rosenkranz, *Adv Eng Mater* **2022**, 2200755.

[29] M. Marian, S. Tremmel, S. Wartzack, G. Song, B. Wang, J. Yu, A. Rosenkranz, *Appl Surf Sci* **2020**, *523*, 146503.

[30] P. Tian, G. Yu, K. Wei, Z. Zhang, N. Wang, *Ceram Int* **2021**, *47*, 30722.

[31] H. Zhang, L. Wang, Q. Chen, P. Li, A. Zhou, X. Cao, Q. Hu, *Mater Des* **2016**, *92*, 682.

[32] X. Zhang, M. Xue, X. Yang, Z. Wang, G. Luo, Z. Huang, X. Sui, C. Li, *RSC Adv* **2015**, *5*, 2762.
[33] S. Yi, Y. Guo, J. Li, Y. Zhang, A. Zhou, J. Luo, *Friction* **2022**.
[34] M. Marian, G.C. Song, B. Wang, V.M. Fuenzalida, S. Krauß, B. Merle, S. Tremmel, S. Wartzack, J. Yu, A. Rosenkranz, *Appl Surf Sci* **2020**, *531*, 147311.
[35] H. Xiao, S. Liu, *Mater Des* **2017**, *135*, 319.
[36] A.A. Mohamed Faruck, C.J. Hsu, N. Doerr, M. Weigand, C. Gachot, *Tribol Int* **2020**, *151*, 106390.
[37] M. Naguib, M. Kurtoglu, V. Presser, J. Lu, J. Niu, M. Heon, L. Hultman, Y. Gogotsi, M.W. Barsoum, *Advanced Materials* **2011**, *23*, 4248.
[38] A. Sarycheva, Y. Gogotsi, *Chemistry of Materials* **2020**, *32*, 3480.
[39] J. Gao, C.-F. Du, T. Zhang, X. Zhang, Q. Ye, S. Liu, W. Liu, *ACS Appl Nano Mater* **2021**, acsanm.1c02556.
[40] S. Chen, Y. Xiang, M.K. Banks, C. Peng, W. Xu, R. Wu, *Nanoscale* **2018**, *10*, 20043.
[41] E.I. Izgorodina, D.R. MacFarlane, *J Phys Chem B* **2011**, *115*, 14659.
[42] Y. Li, Q. Zhang, W. Zhou, Y. Huang, J. Han, *Lubricants* **2023**, *11*, 147.
[43] H. Fang, Y. Li, S. Zhang, Q. Ding, L. Hu, K. Lu, *J Colloid Interface Sci* **2022**, *623*, 257.
[44] S. Kawada, S. Watanabe, C. Tadokoro, S. Sasaki, *Tribol Lett* **2018**, *66*.
[45] M. Cai, Q. Yu, W. Liu, F. Zhou, *Chem Soc Rev* **2020**, *49*, 7753.
[46] R. Kreivaitis, M. Gumbytė, A. Kupčinskas, K. Kazancev, V. Makarevičienė, *Tribol Int* **2020**, *141*.
[47] R.K. Upadhyay, A. Kumar, *Colloids and Interface Science Communications* **2019**, *31*.